



## Full Length Article

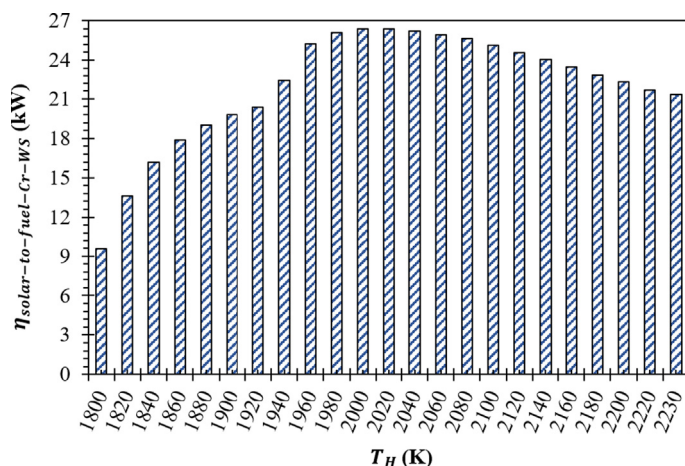
# Application of chromium oxide-based redox reactions for hydrogen production via solar thermochemical splitting of water

Rahul R. Bhosale

Department of Chemical Engineering, College of Engineering, Qatar University, Doha, Qatar



## GRAPHICAL ABSTRACT



## ARTICLE INFO

## Keywords:

Cr<sub>2</sub>O<sub>3</sub>  
Hydrogen  
Water splitting  
Thermodynamics  
Thermal reduction  
Solar-to-fuel energy conversion efficiency

## ABSTRACT

Thermodynamic equilibrium, as well as efficiency analysis of the Cr<sub>2</sub>O<sub>3</sub>/Cr water splitting (Cr-WS) cycle, was conducted in this study. The thermodynamic properties required for the computations were obtained from an HSC Chemistry 9.9 software. An increase in thermal reduction (TR) temperature ( $T_H$ ) from 1800 K to 2230 K was responsible for the rise in the percentage TR of Cr<sub>2</sub>O<sub>3</sub> (Tr-Cr) from 0% to 100%. The equilibrium analysis additionally indicates that the re-oxidation of Cr into Cr<sub>2</sub>O<sub>3</sub> via WS reaction is feasible at any temperature from 300 to 3000 K (we have selected 1300 K for this study). The efficiency analysis indicates that the  $\dot{Q}_{\text{solar-reactor-Cr-WS}}$  and  $\dot{Q}_{\text{solar-heater-Cr-WS}}$  were enhanced by 3636.8 kW and 260.0 kW due to the increment in the  $T_H$  from 1800 K to 2230 K. The increase in the  $\dot{Q}_{\text{solar-reactor-Cr-WS}}$  and  $\dot{Q}_{\text{solar-heater-Cr-WS}}$  resulted into a rise in the  $\dot{Q}_{\text{solar-cycle-Cr-WS}}$  by 3896.8 kW. The  $\eta_{\text{solar-to-fuel-Cr-WS}}$  increased from 9.5% to 26.4% when the  $T_H$  was augmented from 1800 K to 2000 K. A further rise in the  $T_H$  from 2000 K to 2230 K resulted in a reduction in the  $\eta_{\text{solar-to-fuel-Cr-WS}}$  from 26.4% to 21.3%. After employing the 100% heat recuperation, then  $\eta_{\text{solar-to-fuel-HR-Cr-WS}}$  of the Cr-WS cycle was improved up to 48.3% at  $T_H = 2000$  K.

E-mail address: [rahul.bhosale@qu.edu.qa](mailto:rahul.bhosale@qu.edu.qa).

<https://doi.org/10.1016/j.fuel.2020.118160>

Received 28 February 2020; Received in revised form 20 April 2020; Accepted 19 May 2020

0016-2361/ © 2020 Elsevier Ltd. All rights reserved.

## Nomenclature

$C$	Solar flux concentration ratio, suns
$HHV$	Higher heating value, kW
$I$	Normal beam solar insolation, W/m <sup>2</sup>
$MO$	Metal oxide
$\dot{n}$	Molar flow rate, mol/s
$T_H$	TR temperature, K
$T_L$	Water splitting temperature, K
$HR$	Heat recuperation
$P_{O_2}$	The partial pressure of the O <sub>2</sub> in the inert gas, atm
$\sigma$	Stefan – Boltzmann constant, $5.670 \times 10^{-8}$ (W/m <sup>2</sup> ·K <sup>4</sup> )
$\dot{Q}_{Nb_2O_5-red(partial)-Cr-WS}$	Energy required for partially reduce the Cr <sub>2</sub> O <sub>3</sub> , kW
$\dot{Q}_{H_2O-heating-Cr-WS}$	Energy required for the heating of H <sub>2</sub> O, kW
$\dot{Q}_{cycle-net-Cr-WS}$	Net energy required to run the Cr-WS cycle, kW
$\dot{Q}_{solar-reactor-Cr-WS}$	Solar energy required to run the solar reactor, kW
$\dot{Q}_{solar-heater-Cr-WS}$	Solar energy required to run the solar heater, kW
$\dot{Q}_{solar-cycle-Cr-WS}$	Solar energy required to run the Cr-WS cycle, kW
$\eta_{abs-solar-reactor-Cr-WS}$	Solar energy absorption efficiency of the solar reactor, %

$\eta_{abs-solar-heater-Cr-WS}$	Solar energy absorption efficiency of the solar heater, %
$\dot{Q}_{re-rad-solarreactor-Cr-WS}$	Re-radiation losses from the solar reactor, kW
$\dot{Q}_{re-rad-solar-heater-Cr-WS}$	Re-radiation losses from the solar heater, kW
$\dot{Q}_{re-rad-cycle-Cr-WS}$	Re-radiation losses from the Cr-WS cycle, kW
$\dot{Q}_{cooler-1-Cr-WS}$	Energy liberated from cooler – 1, kW
$\dot{Q}_{cooler-2-Cr-WS}$	Energy liberated from cooler – 2, kW
$\dot{Q}_{cooler-3-Cr-WS}$	Energy liberated from cooler – 3, kW
$\dot{Q}_{splitting-reactor-Cr-WS}$	Energy liberated from the WS splitting reactor, kW
$\eta_{solar-to-fuel-Cr-WS}$	Solar-to-fuel energy conversion efficiency of the Cr-WS cycle, %
$\eta_{solar-to-fuel-HR-Cr-WS}$	Solar-to-fuel energy conversion efficiency (with heat recuperation) of the Cr-WS cycle, %
$\dot{Q}_{recuperable-Cr-WS}$	Total energy recuperated from the Cr-WS cycle, kW
$\dot{Q}_{recuperable-HR-Cr-WS}$	Energy recuperated from the Cr-WS cycle (with % HR), kW
$\dot{Q}_{solar-cycle-HR-Cr-WS}$	Solar energy required to run the Cr-WS cycle (with heat recuperation), kW

## 1. Introduction

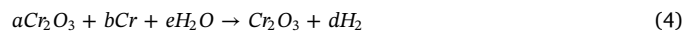
The increase in the demand for energy (current and future) is majorly attributed to the rise in the world's population and CO<sub>2</sub> induced pollution[1–4]. Besides, the environmental pollution occurring due to the excessive utilization of fossil fuels (to fulfill the energy demand) is driving the researchers to find potential and environmentally clean energy sources, which can be considered as future energy supplies [5]. Several researchers believe that H<sub>2</sub> has the potential to replace the fossil fuels provided that it should be produced from clean raw materials, and by utilizing the renewable energy[6]. Hence, several research groups all around the world are focused on solar H<sub>2</sub> production via water splitting (WS) thermochemical cycles[7,8].

A metal oxide (MO) based solar-driven thermochemical WS cycle is considered as one of the promising alternatives for the production of H<sub>2</sub>[9–11]. This cycle requires a lower temperature for the conversion of H<sub>2</sub>O into H<sub>2</sub> as compared to the direct thermolysis. The operation of this cycle is very safe as H<sub>2</sub> and O<sub>2</sub> produced in two separate steps. Besides, the metal oxide can be reutilized for conducting multiple thermochemical cycles. The primary reaction chemistry associated with the Mo-based thermochemical WS cycles is represented below:



In previous studies, two types of MOs, namely, volatile and non-volatile, were examined both experimentally as well as theoretically for the thermochemical H<sub>2</sub> production via WS. The volatile MOs mainly includes ZnO/Zn[12–17] and SnO<sub>2</sub>/SnO/Sn systems[18–21] and the non-volatile MOs were mainly ferrites [22–35], ceria/doped ceria[36–47], perovskites[48–56], and others[57–60]. In most of the studies, a higher thermal reduction (TR) temperature was employed to attain a significant %TR. At these conditions, the phase of the volatile MOs changed from solid to gas, whereas the non-volatile MOs remained either in solid or solid solution phase. One of the major objectives of these studies was to attain a higher level of fuel production at the lowest possible operating temperatures. From the obtained results, it was understood that to achieve a higher fuel production, the extent of TR of the MOs needs to be elevated. To achieve an eminent TR, the MO needs to be reduced at a higher temperature. Because of the requirement of the higher TR temperature, the solar energy input required to drive the solar reactor was augmented, and hence the  $\eta_{solar-to-fuel}$  was lowered.

It is believed that the complete TR of MO may not be necessarily required to achieve the highest possible  $\eta_{solar-to-fuel}$ . The partial TR of MO is possible at lower temperatures, and hence the overall supply of the solar energy needed to drive the solar reactor can be lowered. To explore these options, in this investigation, we have thermodynamically scrutinized the Cr<sub>2</sub>O<sub>3</sub>/Cr based WS (Cr-WS) cycle by assuming partial TR of the Cr<sub>2</sub>O<sub>3</sub>. Cr has been applied as a catalyst for the production of H<sub>2</sub> via the sulfur-iodine cycle[61] and the photochemical splitting of H<sub>2</sub>O[62]. Likewise, it was used as an active dopant for ceria based thermochemical WS cycle[63]. Cr has been used for H<sub>2</sub> production via thermochemical and photochemical pathways. However, the utilization of the Cr-based oxides towards the MO-based thermochemical WS cycle is not yet investigated. The redox reactions associated with the Cr-WS (by assuming partial TR) are as follows:



## 2. Estimation of equilibrium compositions

In this investigation, the thermodynamic process parameters associated with the Cr-WS cycle were calculated. The efficiency analysis was conducted by using the HSC Chemistry 9.1 software and its thermodynamic database. The efficiency analysis calculations (reported in section 3 and 4) considerably depends on a) the equilibrium compositions and b) the temperatures associated with any thermochemical cycle.  $\eta_{solar-to-fuel-Nb-WS}$  Therefore, before performing any efficiency-related calculations, the equilibrium compositions and the TR ( $T_H$ ) and WS ( $T_L$ ) temperatures associated with the Cr-WS cycle were estimated. To maintain the reaction conditions identical to the previously investigated thermochemical cycles, all computations related to the equilibrium compositions were carried out at  $P_{O_2} = 10^{-6}$  atm. The equilibrium compositions associated with the TR steps were estimated by selecting the following species from the HSC Chemistry database: Cr<sub>2</sub>O<sub>3</sub>(s), CrO<sub>2</sub>(g), CrO(g), Cr(s), Cr(g), and O<sub>2</sub>(g). According to the thermodynamic understanding, the CrO<sub>2</sub> decomposes into Cr and O<sub>2</sub> above 650 K. Hence, to avoid confusion and to provide reliable results, the CrO<sub>2</sub>(s) and CrO<sub>2</sub>(g) were excluded from the equilibrium analysis. The equilibrium compositions associated with the TR of Cr<sub>2</sub>O<sub>3</sub> (after the exclusion of CrO<sub>2</sub>) were obtained from the HSC Chemistry software and reported in Fig. 1 (as a function of the variation in the  $T_H$ ). A close inspection of the plots associated with the equilibrium compositions

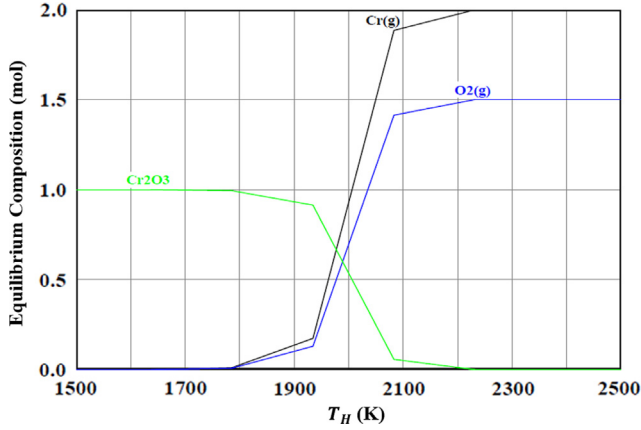


Fig. 1. Effect of  $T_H$  on the equilibrium compositions of the TR of  $\text{Cr}_2\text{O}_3$  (at  $P_{\text{O}_2} = 10^{-6}$  atm).

clearly shows that the TR of  $\text{Cr}_2\text{O}_3$  was initiated at  $T_H$  equal to 1760 K. Furthermore, the equilibrium analysis indicate that the 100% TR of  $\text{Cr}_2\text{O}_3$  into  $\text{Cr}(\text{g})$  and  $\text{O}_2(\text{g})$  can be attained if the solar reactor is heated up to a  $T_H$  of 2230 K.

As mentioned in the introduction section, this study was conducted to identify the influence of partial TR of  $\text{Cr}_2\text{O}_3$  on the solar-to-fuel energy conversion efficiency ( $\eta_{\text{solar-to-fuel-Cr-WS}}$ ) of the Cr-WS cycle. Therefore, it was essential first to identify the relation between the  $T_H$  and the percentage partial TR of Cr-WS (%TR-Cr). By utilizing the results obtained during the equilibrium analysis, %TR-Cr was estimated as a function of the rise in  $T_H$ . Variations associated with %TR-Cr due to the upsurge in  $T_H$  from 1800 K to 2230 K are reported in Fig. 2. The trends reported shows that the %TR-Cr was increased in three zones due to the increment in the  $T_H$  from 1800 K to 2230 K. When the  $T_H$  was increased from 1800 K to 1920 K (zone-1), a slow rise in the TR-Cr from 1.3% to 7.9% was observed. As the  $T_H$  was augmented from 1920 K to 2100 K (zone-2), the TR-Cr was quickly rose from 7.9% up to 94.9%. Again a sluggish surge in the TR-Cr from 94.9% up to 100% was noticed when the  $T_H$  was increased from 1920 K to 2230 K (zone-3). These results indicate that the influence of the rise in  $T_H$  on %TR-Cr was considered significant in zone-2 when compared to zone-1 and zone-3.

In addition to  $T_H$ , the temperature above which the WS reaction is likely needed to be estimated as well.  $T_L$ . The determination of the  $T_L$  at which the re-oxidation of Cr via WS reaction is possible was carried out by exploring the variation in the delta G. The delta G values obtained as a function of the change in the  $T_L$  are reported in Fig. 3. In terms of numbers, the delta G was increased from  $-372.1$  kJ/mol to  $-298.2$  kJ/mol,  $-218.2$  kJ/mol, and  $-137.4$  kJ/mol when the  $T_L$  was augmented from 300 K to 1000 K, 2000 K, and 3000 K, respectively. The reported results indicate that at all  $T_L$  values, the delta G associated with the WS reaction was negative (below zero). As per the variations allied with delta G, WS reaction via re-oxidation of Cr is feasible at all temperatures below 3000 K. Although the WS is feasible at all  $T_L$ , based on the experimental conditions considered in the previous investigations [42,64], the WS reaction allied with the Cr-WS cycle was performed at 1300 K ( $\sim 1000^\circ\text{C}$ ).

### 3. Efficiency analysis: Methodology and equations

After estimating the equilibrium compositions, a process flow configuration for the Cr-WS cycle was developed (Fig. 4). This process flow configuration, which includes both solar-driven and non-solar driven equipment, was considered as the basis for the efficiency analysis allied with the Cr-WS cycle. In addition to the process flow configuration presented in Fig. 5, the following essential assumptions were employed for solving the equations associated with the efficiency analysis.

- A continuous feed flow of  $\text{Cr}_2\text{O}_3$  (1 mol/s)
- The solar-driven equipments were well insulated towards conductive and convective heat losses
- WS reaction was assumed to be completed with 100% conversion rate
- Negligible variations in the potential and kinetic energies
- Natural separation of the products
- Heat exchangers are neglected during the efficiency analysis

The solar reactor and the solar heater are the two major equipments installed in the cycle, which was driven by using concentrated solar power. The  $\dot{Q}_{\text{solar-reactor-Cr-WS}}$  and  $\dot{Q}_{\text{solar-heater-Cr-WS}}$  were computed as:

$$\dot{Q}_{\text{solar-reactor-Cr-WS}} = \frac{\dot{Q}_{\text{Cr}_2\text{O}_3\text{-red (partial)-Cr-WS}}}{\eta_{\text{abs-solar-reactor-Cr-WS}}} \quad (5)$$

$$\dot{Q}_{\text{solar-heater-Cr-WS}} = \frac{\dot{Q}_{\text{H}_2\text{O-heating-Cr-WS}}}{\eta_{\text{abs-solar-steamgenerator-Cr-WS}}} \quad (6)$$

To solve Eqs. (5) and (6), it was essential to determine the solar energy absorption efficiencies of the solar reactor and solar heater.

$$\eta_{\text{abs-solar-reactor-Cr-WS}} = 1 - \left( \frac{\sigma T_H^4}{IC} \right) \quad (7)$$

$$\eta_{\text{abs-solar-steamgenerator-Cr-WS}} = 1 - \left( \frac{\sigma T_L^4}{IC} \right) \quad (8)$$

Where,  $I = 1000 \text{ W/m}^2$ ,  $C = 3000 \text{ suns}$ ,  $\sigma = 5.670 \times 10^{-8} \text{ W/m}^2\text{K}^4$ .

Similarly, the energy needed to a) perform the TR step and b) produce and heat the steam to the desired temperature was also calculated as per the following equations.

$$\dot{Q}_{\text{Cr}_2\text{O}_3\text{-red (partial)-Cr-WS}} = \dot{n}\Delta H_{\text{Cr}_2\text{O}_3(\text{s})@T_L \rightarrow a\text{Cr}_2\text{O}_3(\text{s})+b\text{Cr}(\text{g})+c\text{O}_2(\text{g})@T_H} \quad (9)$$

$$\dot{Q}_{\text{H}_2\text{O-heating-Cr-WS}} = \dot{n}\Delta H_{\text{eH}_2\text{O}(\text{l})@298\text{K} \rightarrow \text{eH}_2\text{O}(\text{g})@T_L} \quad (10)$$

By utilizing Eqs. (9) and (10), the  $\dot{Q}_{\text{cycle-net-Cr-WS}}$  was computed as:

$$\dot{Q}_{\text{cycle-net-Cr-WS}} = \dot{Q}_{\text{Cr}_2\text{O}_3\text{-red (partial)-Cr-WS}} + \dot{Q}_{\text{H}_2\text{O-heating-Cr-WS}} \quad (11)$$

Likewise, the  $\dot{Q}_{\text{solar-cycle-Cr-WS}}$  was valued by the utilization of the data obtained via Eqs. (5) and (6).

$$\dot{Q}_{\text{solar-cycle-Cr-WS}} = \dot{Q}_{\text{solar-reactor-Cr-WS}} + \dot{Q}_{\text{solar-heater-Cr-WS}} \quad (12)$$

Although the walls of the solar reactor and solar heater were well insulated, the heat losses from these two equipment's due to the re-radiation were unavoidable and hence computed as follows:

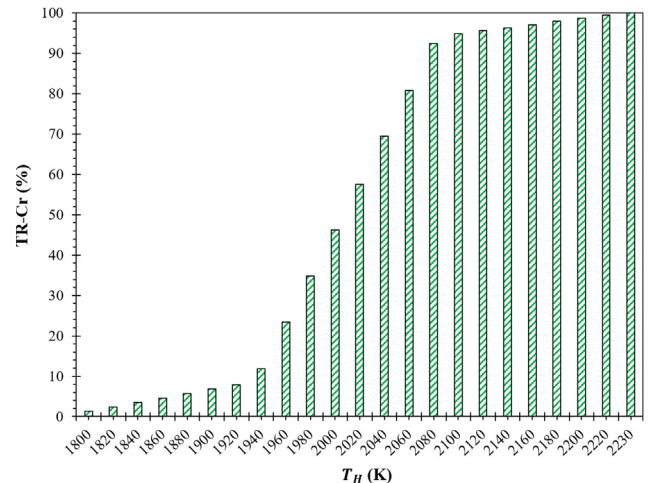


Fig. 2. Effect of  $T_H$  on %TR-Cr (at  $P_{\text{O}_2} = 10^{-6}$  atm).

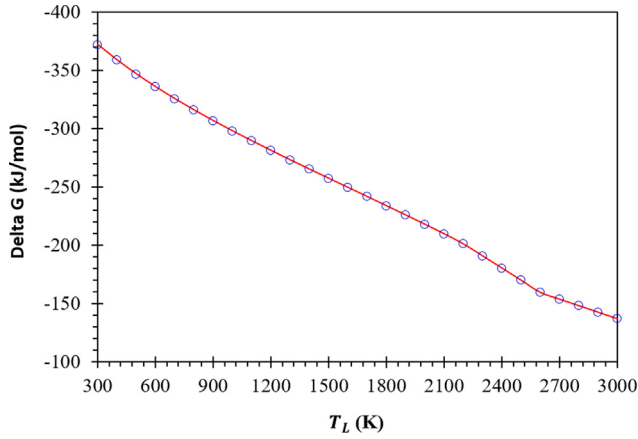


Fig. 3. Effect of  $T_L$  on delta G associated with the WS reaction (Cr-WS cycle).

$$\dot{Q}_{re-rad-solar-reactor-Cr-WS} = \dot{Q}_{solar-reactor-Cr-WS} - \dot{Q}_{Cr_2O_3-red(partial)-Cr-WS} \quad (13)$$

$$\dot{Q}_{re-rad-solar-heater-Cr-WS} = \dot{Q}_{solar-heater-Cr-WS} - \dot{Q}_{H_2O-heating-Cr-WS} \quad (14)$$

With the help of Eqs. (13) and (14), the overall heat losses from the Cr-WS cycle due to re-radiation were estimated as per the following expression.

$$\dot{Q}_{re-rad-cycle-Cr-WS} = \dot{Q}_{re-rad-solar-reactor-Cr-WS} + \dot{Q}_{re-rad-solar-heater-Cr-WS} \quad (15)$$

Three coolers were installed in the Cr-WS cycle for reducing the temperatures of a) products of the TR reaction, b)  $O_2$  separated from the TR products, and c) the  $H_2$  produced via WS reaction.

$$\dot{Q}_{cooler-1-Cr-WS} = -\dot{n}\Delta H|_{aCr_2O_3(s)+bCr(g)+cO_2(g)@T_H \rightarrow aCr_2O_3(s)+bCr(s)+cO_2(g)@T_L} \quad (16)$$

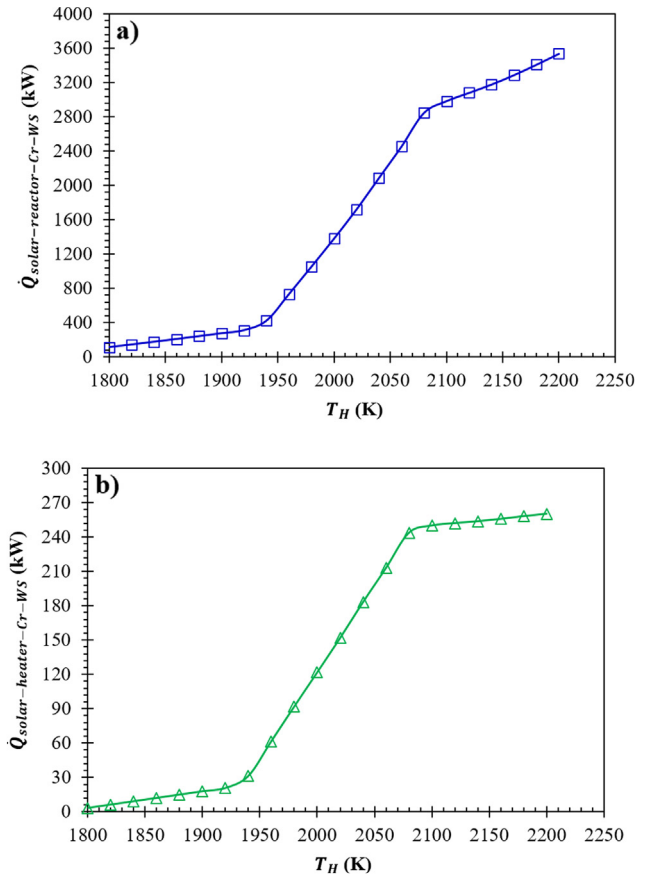


Fig. 5. Effect of  $T_H$  on a)  $\dot{Q}_{solar-reactor-Cr-WS}$  and b)  $\dot{Q}_{solar-heater-Cr-WS}$  ( $T_L = 1300$  K).

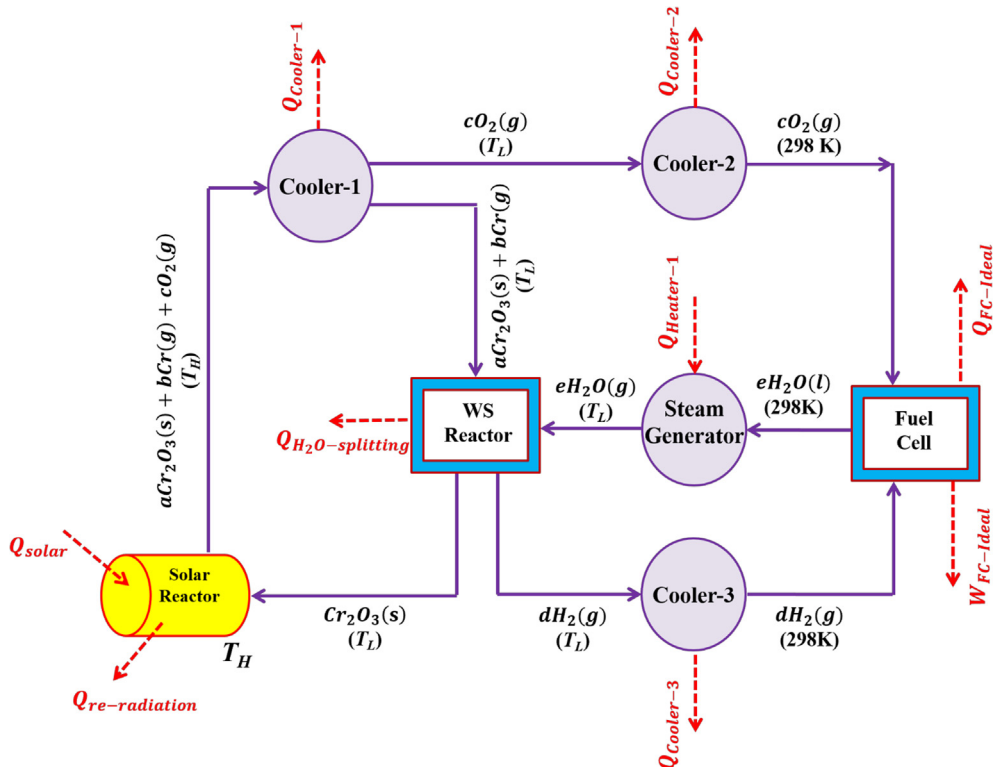


Fig. 4. Process flow configuration of the Cr-WS cycle.

$$\dot{Q}_{\text{cooler}-2-\text{Cr}-\text{WS}} = -\dot{n}\Delta H|_{\text{CO}_2(\text{g})@T_L \rightarrow \text{CO}_2(\text{g})@298\text{K}} \quad (17)$$

$$\dot{Q}_{\text{cooler}-3-\text{Cr}-\text{WS}} = -\dot{n}\Delta H|_{\text{dH}_2(\text{g})@T_L \rightarrow \text{dH}_2(\text{g})@298\text{K}} \quad (18)$$

In addition to the high-temperature solar-driven cavity-based reactor (utilized for performing the TR reactions), a non-solar driven WS reactor was also installed in the cycle. Due to the exothermic nature of the WS reaction, the heat energy released from the WS reactor was estimated as:

$$\dot{Q}_{\text{splitting}-\text{reactor}-\text{Cr}-\text{WS}} = -\dot{n}\Delta H|_{\text{aCr}_2\text{O}_3(\text{s})+\text{bCr}(\text{s})+\text{eH}_2\text{O}(\text{g})@T_L \rightarrow \text{Cr}_2\text{O}_3(\text{s})+\text{dH}_2(\text{g})@T_L} \quad (19)$$

The results obtained by solving the Eqs. (16) to (19) were combined for the estimation of the amount of heat energy that can be recuperated from the Cr-WS cycle.

$$\begin{aligned} \dot{Q}_{\text{recuperable}-\text{Cr}-\text{WS}} &= \dot{Q}_{\text{cooler}-1-\text{Cr}-\text{WS}} + \dot{Q}_{\text{cooler}-2-\text{Cr}-\text{WS}} + \dot{Q}_{\text{cooler}-3-\text{Cr}-\text{WS}} \\ &+ \dot{Q}_{\text{splitting}-\text{reactor}-\text{Cr}-\text{WS}} \end{aligned} \quad (20)$$

The role of the recuperation was to reduce the solar energy required to drive the Cr-WS cycle. Hence, after employing the heat recuperation, the new  $\dot{Q}_{\text{solar}-\text{cycle}-\text{HR}-\text{Cr}-\text{WS}}$  was calculated by utilizing the following equations.

$$\dot{Q}_{\text{solar}-\text{cycle}-\text{HR}-\text{Cr}-\text{WS}} = \dot{Q}_{\text{solar}-\text{cycle}-\text{Cr}-\text{WS}} - \dot{Q}_{\text{recuperable}-\text{HR}-\text{Cr}-\text{WS}} \quad (21)$$

Where

$$\dot{Q}_{\text{recuperable}-\text{HR}-\text{Cr}-\text{WS}} = (\% \text{HR}) \times \dot{Q}_{\text{recuperable}-\text{Cr}-\text{WS}} \quad (22)$$

The amount of heat released and work done by the fuel cell was also calculated by using Eqs. (23) and (24).

$$\dot{W}_{\text{FC}-\text{Ideal}-\text{Cr}-\text{WS}} = -\dot{n}\Delta G|_{\text{dH}_2(\text{g})+\text{cO}_2(\text{g})@298\text{K} \rightarrow \text{eH}_2\text{O}(\text{l})@298\text{K}} \quad (23)$$

$$\dot{Q}_{\text{FC}-\text{Ideal}-\text{Cr}-\text{WS}} = -(298) \times \dot{n}\Delta S|_{\text{dH}_2(\text{g})+\text{cO}_2(\text{g}) \rightarrow \text{eH}_2\text{O}(\text{l})@298\text{K}} \quad (24)$$

The feasibility of the Cr-WS cycle was estimated by calculating the  $\eta_{\text{solar}-\text{to}-\text{fuel}-\text{Cr}-\text{WS}}$ .

$$\eta_{\text{solar}-\text{to}-\text{fuel}-\text{Cr}-\text{WS}} = \frac{\text{HHV}_{\text{H}_2} \times (\text{moles of H}_2 \text{ produced})}{\dot{Q}_{\text{solar}-\text{cycle}-\text{Cr}-\text{WS}}} \quad (25)$$

Besides, the effect of HR on the Cr-WS cycle was scrutinized by estimating the  $\eta_{\text{solar}-\text{to}-\text{fuel}-\text{HR}-\text{Cr}-\text{WS}}$ .

$$\eta_{\text{solar}-\text{to}-\text{fuel}-\text{HR}-\text{Cr}-\text{WS}} = \frac{\text{HHV}_{\text{H}_2} \times (\text{moles of H}_2 \text{ produced})}{\dot{Q}_{\text{solar}-\text{cycle}-\text{HR}-\text{Cr}-\text{WS}}} \quad (26)$$

The preciseness of the thermodynamic analysis was scrutinized by comparing the  $\dot{W}_{\text{FC}-\text{Ideal}-\text{Cr}-\text{WS}}$  calculated by Eqs. (23) with Eqs. (27).

$$\begin{aligned} \dot{W}_{\text{FC}-\text{Ideal}-\text{Cr}-\text{WS}} &= \dot{Q}_{\text{solar}-\text{cycle}-\text{Cr}-\text{WS}} - \\ &(\dot{Q}_{\text{re-rad}-\text{cycle}-\text{Cr}-\text{WS}} + \dot{Q}_{\text{cooler}-1-\text{Cr}-\text{WS}} + \dot{Q}_{\text{cooler}-2-\text{Cr}-\text{WS}} \\ &+ \dot{Q}_{\text{cooler}-3-\text{Cr}-\text{WS}} + \dot{Q}_{\text{splitting}-\text{reactor}-\text{Cr}-\text{WS}} + \dot{Q}_{\text{FC}-\text{Ideal}-\text{Cr}-\text{WS}}) \end{aligned} \quad (27)$$

#### 4. Efficiency analysis: Results and discussion

As the second phase of this analysis, with the help of the equilibrium compositions (presented in section 2) and the thermodynamic calculations (presented in section 3), the efficiency analysis of the Cr-WS cycles were carried out. These efficiency analysis calculations were conducted to estimate the %TR-Cr at which the Cr-WS cycle attains the maximum possible  $\eta_{\text{solar}-\text{to}-\text{fuel}-\text{Cr}-\text{WS}}$ .

Two of the principal parameters on which the cycle efficiency depends are the  $\dot{Q}_{\text{solar}-\text{reactor}-\text{Cr}-\text{WS}}$  and  $\dot{Q}_{\text{solar}-\text{heater}-\text{Cr}-\text{WS}}$ . However, to estimate these two parameters, it was first essential to calculate the  $\dot{Q}_{\text{Cr}_2\text{O}_3-\text{red}(\text{partial})-\text{Cr}-\text{WS}}$  and  $\dot{Q}_{\text{H}_2\text{O}-\text{heating}-\text{Cr}-\text{WS}}$ . By varying the  $T_H$ , the

**Table 1**

Effect of  $T_H$  on the  $\dot{Q}_{\text{Cr}_2\text{O}_3-\text{red}(\text{partial})-\text{Cr}-\text{WS}}$  and  $\dot{Q}_{\text{H}_2\text{O}-\text{heating}-\text{Cr}-\text{WS}}$  ( $T_L = 1300$  K).

$T_H$ (K)	$\dot{Q}_{\text{Cr}_2\text{O}_3-\text{red}(\text{partial})-\text{Cr}-\text{WS}}$ (kW)	$\dot{Q}_{\text{H}_2\text{O}-\text{heating}-\text{Cr}-\text{WS}}$ (kW)
1800	91.0	3.2
1820	114.4	6.0
1840	137.9	8.7
1860	161.3	11.5
1880	184.7	14.2
1900	208.1	16.9
1920	231.5	19.7
1940	309.4	29.6
1960	528.2	58.3
1980	747.0	87.0
2000	961.8	115.1
2020	1178.3	143.5
2040	1404.1	173.2
2060	1618.5	201.3
2080	1839.9	230.4
2100	1887.3	236.4
2120	1904.5	238.4
2140	1918.3	240.0
2160	1935.1	241.9
2180	1954.1	244.2
2200	1971.1	246.1
2220	1987.3	248.0
2230	1997.2	249.2

$\dot{Q}_{\text{Cr}_2\text{O}_3-\text{red}(\text{partial})-\text{Cr}-\text{WS}}$  and  $\dot{Q}_{\text{H}_2\text{O}-\text{heating}-\text{Cr}-\text{WS}}$  were computed by utilizing the Eqs. (9) and (10) and the obtained results are reported in Table 1. As the  $T_H$  was increased from 1800 K to 2230 K, the enthalpy of Cr(g), and O<sub>2</sub>(g) was also augmented by 868.1 kW and 100.9 kW, respectively. As the enthalpies of the products increased, the  $\dot{Q}_{\text{Cr}_2\text{O}_3-\text{red}(\text{partial})-\text{Cr}-\text{WS}}$  was also enhanced by a factor of 21.9.

As per Eq. (6), the  $\dot{Q}_{\text{solar}-\text{heater}-\text{Cr}-\text{WS}}$  can be computed by dividing the  $\dot{Q}_{\text{H}_2\text{O}-\text{heating}-\text{Cr}-\text{WS}}$  by  $\eta_{\text{abs}-\text{solar}-\text{heater}-\text{Cr}-\text{WS}}$ . As per the data reported in Table 1, the  $\dot{Q}_{\text{H}_2\text{O}-\text{heating}-\text{Cr}-\text{WS}}$  was augmented from 3.2 kW to 249.2 kW when the  $T_H$  was enhanced from 1800 K to 2230 K. Opposite to this; the  $\eta_{\text{abs}-\text{solar}-\text{heater}-\text{Cr}-\text{WS}}$  was observed to be steady at 94.6% because the  $T_L$  was kept constant at 1300 K. As the numerator value was increased and the denominator value is steady, the  $\dot{Q}_{\text{solar}-\text{heater}-\text{Cr}-\text{WS}}$  was augmented from 3.4 kW to 263.4 kW as a function of the rise in the  $T_H$  from 1800 K to 2230 K (Fig. 5b). As the  $\dot{Q}_{\text{solar}-\text{reactor}-\text{Cr}-\text{WS}}$  and  $\dot{Q}_{\text{solar}-\text{heater}-\text{Cr}-\text{WS}}$  primarily depend upon the %TR-Cr, they have followed the trend identical to the one reported in the case of the rise in the %TR-Cr (Fig. 2).

Estimation of the  $\dot{Q}_{\text{cycle}-\text{net}-\text{Cr}-\text{WS}}$  is vital to identify the amount of heat energy required to drive the cycle (neglecting the re-radiation losses). According to Eq. (11), the  $\dot{Q}_{\text{cycle}-\text{net}-\text{Cr}-\text{WS}}$  is the summation of  $\dot{Q}_{\text{Cr}_2\text{O}_3-\text{red}(\text{partial})-\text{Cr}-\text{WS}}$  and  $\dot{Q}_{\text{H}_2\text{O}-\text{heating}-\text{Cr}-\text{WS}}$ . As both  $\dot{Q}_{\text{Cr}_2\text{O}_3-\text{red}(\text{partial})-\text{Cr}-\text{WS}}$  and  $\dot{Q}_{\text{H}_2\text{O}-\text{heating}-\text{Cr}-\text{WS}}$  were increased, the  $\dot{Q}_{\text{cycle}-\text{net}-\text{Cr}-\text{WS}}$  was also augmented as a function of the rise in the  $T_H$ . The numbers listed in Table 2 shows that the  $\dot{Q}_{\text{cycle}-\text{net}-\text{Cr}-\text{WS}}$  was increased from 94.2 kW up to 1076.9 kW and 2246.4 kW when the  $T_H$  was upscaled from 1800 K to 2000 K, and 230 K, respectively. Table 2 also represents the increment in the  $\dot{Q}_{\text{solar}-\text{cycle}-\text{Cr}-\text{WS}}$  by a factor of 34.3 due to the upsurge in the  $T_H$  from 1800 K to 2230 K. Similar to the  $\dot{Q}_{\text{cycle}-\text{net}-\text{Cr}-\text{WS}}$ , the  $\dot{Q}_{\text{solar}-\text{cycle}-\text{Cr}-\text{WS}}$  was augmented due to the rise in the  $\dot{Q}_{\text{solar}-\text{reactor}-\text{Cr}-\text{WS}}$  and  $\dot{Q}_{\text{solar}-\text{heater}-\text{Cr}-\text{WS}}$ .

Results presented in Table 2 indicate that the  $\dot{Q}_{\text{solar}-\text{reactor}-\text{Cr}-\text{WS}}$  is higher than the  $\dot{Q}_{\text{cycle}-\text{net}-\text{Cr}-\text{WS}}$  at all  $T_H$ . This means, as compared to the required heat supply, a higher solar energy input was required to drive the Cr-WS cycle. The higher solar energy supply was needed to deal with the re-radiation losses from the solar reactor as well as the solar heater. Although the walls of these equipments were very well insulated, the re-radiation losses from the cavity window were inevitable. To understand the quantity of heat lost due to the re-radiation effect, by utilizing Eqs. (13) as well as (14), the  $\dot{Q}_{\text{re-rad}-\text{solar}-\text{reactor}-\text{Cr}-\text{WS}}$  and  $\dot{Q}_{\text{re-rad}-\text{solar}-\text{heater}-\text{Cr}-\text{WS}}$  were calculated.

**Table 2**  
Effect of  $T_H$  on the  $\dot{Q}_{\text{solar-cycle-Cr-WS}}$  and  $\dot{Q}_{\text{solar-cycle-Cr-WS}}$  ( $T_L = 1300$  K).

$T_H$ (K)	$\dot{Q}_{\text{cycle-net-Cr-WS}}$ (kW)	$\dot{Q}_{\text{solar-cycle-Cr-WS}}$ (kW)
1800	94.2	116.9
1820	120.4	150.7
1840	146.6	185.2
1860	172.7	220.5
1880	198.9	256.8
1900	225.0	294.0
1920	251.1	332.3
1940	339.0	453.9
1960	586.6	794.3
1980	833.9	1144.8
2000	1076.9	1500.5
2020	1321.9	1871.2
2040	1577.3	2270.6
2060	1819.9	2666.6
2080	2070.3	3090.9
2100	2123.7	3234.4
2120	2142.9	3332.9
2140	2158.3	3432.0
2160	2177.0	3543.7
2180	2198.3	3668.0
2200	2217.2	3797.7
2220	2235.3	3936.5
2230	2246.4	4013.8

Results presented in Fig. 6 shows that the  $\dot{Q}_{\text{re-rad-solar-reactor-Cr-WS}}$  was higher than the  $\dot{Q}_{\text{re-rad-solar-heater-Cr-WS}}$  at all  $T_H$ . This is an expected observation as the quantity of heat energy supplied to the solar reactor was significantly higher than the heat supplied to the solar heater. Hence, the chances of having upper re-radiation losses from the solar reactor as compared to the solar heater were higher. In terms of numbers, at  $T_H$  equal to 1800 K, 2000 K, and 2230 K, the  $\dot{Q}_{\text{re-rad-solar-reactor-Cr-WS}}$  was higher than the  $\dot{Q}_{\text{re-rad-solar-heater-Cr-WS}}$  by 22.3 kW, 410.4 kW, and 1738.9 kW, respectively. Overall, the  $\dot{Q}_{\text{re-rad-solar-reactor-Cr-WS}}$  and  $\dot{Q}_{\text{re-rad-solar-heater-Cr-WS}}$  were augmented by 1730.6 kW and 14.1 kW when the  $T_H$  was increased from 1800 K to 2230 K.

In addition to the individual  $\dot{Q}_{\text{re-rad-solar-reactor-Cr-WS}}$  and  $\dot{Q}_{\text{re-rad-solar-heater-Cr-WS}}$ , estimation of the  $\dot{Q}_{\text{re-rad-cycle-Cr-WS}}$  was essential to verify the thermodynamic analysis conducted [please check Eq. (17)]. Therefore, by utilizing Eq. (15), the  $\dot{Q}_{\text{re-rad-cycle-Cr-WS}}$  was computed. As per Eq. (15), the  $\dot{Q}_{\text{re-rad-cycle-Cr-WS}}$  is equal to the sum of  $\dot{Q}_{\text{re-rad-solar-reactor-Cr-WS}}$  and  $\dot{Q}_{\text{re-rad-solar-heater-Cr-WS}}$ . Hence, the  $\dot{Q}_{\text{re-rad-cycle-Cr-WS}}$  was enhanced as a function of the rise in the  $T_H$ . For example,  $\dot{Q}_{\text{re-rad-cycle-Cr-WS}}$  was increased by a factor of 77.8 due to the increment in  $T_H$  from 1800 K to 2230 K.

In addition to the solar-driven reactor and heater, a non-solar driven WS reactor was also installed in the Cr-WS cycle. The purpose of this reactor was to host the reaction between the Cr-based species with steam at 1300 K. As the WS reaction is exothermic, the WS reactor emits  $\dot{Q}_{\text{splitting-reactor-Cr-WS}}$  to the surrounding. As per the basics associated with the MO-based thermochemical cycles, higher  $T_H$  is responsible for elevated levels of  $O_2$  release from the MO during the TR step. The quantity of  $H_2$  that can be produced (by assuming a 100% conversion rate) during the WS step relies significantly on the amount of  $O_2$  released during the TR step. Hence, as  $T_H$  increased, the extent of the WS reaction was also enhanced, and the exothermic heat released during this step was augmented. Table 3 reports the influence of  $T_H$  on variations allied with the  $\dot{Q}_{\text{splitting-reactor-Cr-WS}}$ . The outcome of solving the Eq. (19) shows that the  $\dot{Q}_{\text{splitting-reactor-Cr-WS}}$  was increased from 4.9 kW to 377.2 kW due to the upsurge in the  $T_H$  from 1800 K to 2230 K ( $T_L$  was kept constant at 1300 K).

The equipments installed in the Cr-WS cycle were operated at a temperature different than each other. For example, the solar reactor was operated in the range of 1800 K to 2230 K, the WS reactor operated at 1300 K, and the fuel cell was operated at 298 K. Because of this

difference in the operating temperatures, multiple coolers were installed in the Cr-WS cycle. Cooler-1 was placed in the cycle to reduce the temperature of the products associated with the TR step from  $T_H$  to  $T_L$ . To attain a higher  $H_2$  production, the  $T_H$  at which the solar reactor was operated was increased from 1800 K to 2230 K. This rise in the  $T_H$  was responsible for the upsurge in the temperature gas between the  $T_H$  and  $T_L$ . As the temperature gas increased, a higher level of heat energy was released from the cooler-1 during the cooling of the products associated with the TR step. Hence, in terms of numbers, the  $\dot{Q}_{\text{cooler-1-Cr-WS}}$  was enhanced by 795.5 kW when the  $T_H$  was augmented from 1800 K to 2230 K.

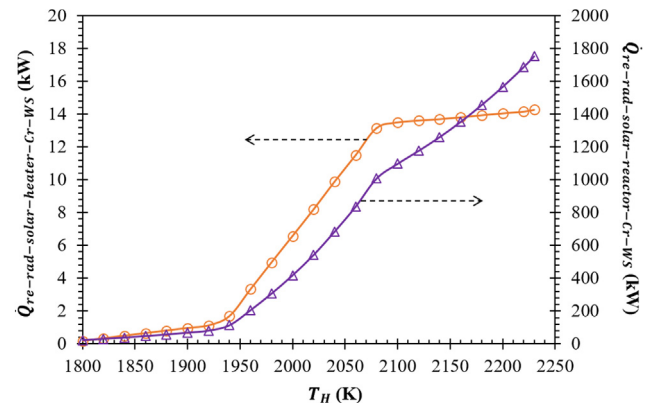
In addition to cooling the products associated with the TR step, cooler-1 plays the role of the separator in which the solid and gaseous products separated naturally. The  $O_2(g)$  coming out from the cooler-1 was further processed in cooler-2 for further reduction in the temperature from  $T_L$  to 298 K. In addition to the  $O_2(g)$ ,  $H_2(g)$  is also essential for the operation of the  $H_2/O_2$  fuel cell. Hence, as the fuel cell was operated at 298 K, alike  $O_2(g)$ , the  $H_2(g)$  was also cooled down from  $T_L$  to 298 K.

Although the inlet and outlet temperature of both cooler-1 and cooler-2 are stable, the increase in the molar concentration of  $O_2(g)$  (due to the rise in %TR-Cr) and  $H_2(g)$  (due to the improvement in the extent of the WS reaction) as a function of  $T_H$  was responsible for the increment in both  $\dot{Q}_{\text{cooler-2-Cr-WS}}$  and  $\dot{Q}_{\text{cooler-3-Cr-WS}}$ .  $\dot{Q}_{\text{cooler-2-Cr-WS}}$  and the  $\dot{Q}_{\text{cooler-3-Cr-WS}}$  were enhanced by 49.4 kW and 88.6 kW with an increase in the  $T_H$  from 1800 K to 2230 K.

By utilizing Eqs. (23) and (24), the  $\dot{W}_{FC-Ideal-Cr-WS}$  and  $\dot{Q}_{FC-Ideal-Cr-WS}$  were estimated. According to the equations, both  $\dot{W}_{FC-Ideal-Cr-WS}$  and  $\dot{Q}_{FC-Ideal-Cr-WS}$  depends upon the quantity of  $H_2$  produced in the Cr-WS cycle. As mentioned earlier, the rise in the  $T_H$  was responsible for the increment in the  $H_2$  produced. Therefore, the increase in the  $T_H$  resulted in the upsurge in the  $\dot{W}_{FC-Ideal-Cr-WS}$  and  $\dot{Q}_{FC-Ideal-Cr-WS}$ . In terms of numbers (Fig. 7), the  $\dot{W}_{FC-Ideal-Cr-WS}$  was augmented by 702.2 kW, and the  $\dot{Q}_{FC-Ideal-Cr-WS}$  was increased by 144.1 kW due to the upsurge in the  $T_H$  from 1800 K to 2230 K.

As the prime aim of this manuscript, by using the data obtained in the thermodynamic analysis and explicitly utilizing the Eq. (25), then  $\eta_{\text{solar-to-fuel-Cr-WS}}$  was calculated. Fig. 8 represent the effect of the rise in the  $T_H$  from 1800 K to 2230 K on  $\eta_{\text{solar-to-fuel-Cr-WS}}$ . The trends reported in Fig. 8 shows that the  $\eta_{\text{solar-to-fuel-Cr-WS}}$  reached the peak value at  $T_H$  equal to 2000 K (TR-Cr = 46.2%) and then started to decrease with the further upsurge in the  $T_H$ . In terms of numbers,  $\eta_{\text{solar-to-fuel-Cr-WS}}$  increased from 9.5% to 26.4% when the  $T_H$  was augmented from 1800 K to 2000 K. A further rise in the  $T_H$  from 2000 K to 2230 K resulted in a reduction in the  $\eta_{\text{solar-to-fuel-Cr-WS}}$  from 26.4% to 21.3%.

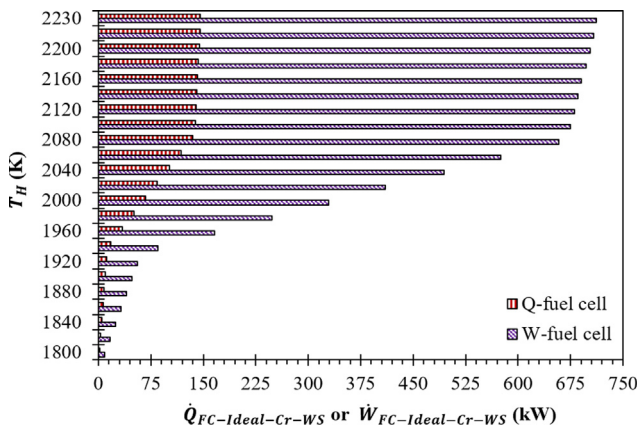
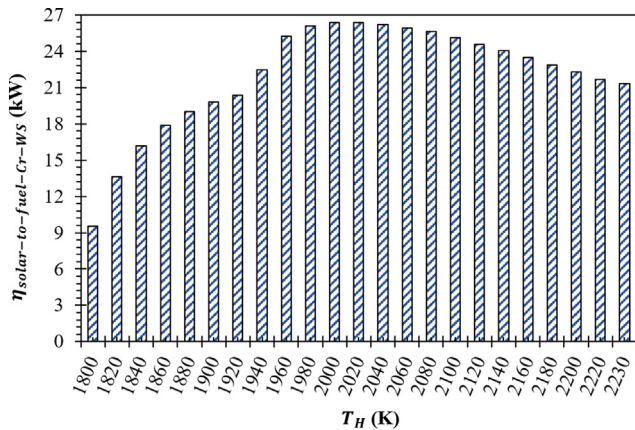
It is interesting to know why such increasing and then decreasing trend was observed in the case of  $\eta_{\text{solar-to-fuel-Cr-WS}}$ . During the initial



**Fig. 6.** Effect of  $T_H$  on  $\dot{Q}_{\text{re-rad-solar-reactor-Cr-WS}}$  and  $\dot{Q}_{\text{re-rad-solar-heater-Cr-WS}}$  ( $T_L = 1300$  K).

**Table 3**Effect of  $T_H$  on  $\dot{Q}_{\text{cooler-1-Cr-WS}}$ ,  $\dot{Q}_{\text{cooler-2-Cr-WS}}$ ,  $\dot{Q}_{\text{cooler-3-Cr-WS}}$ , and  $\dot{Q}_{\text{splitting-reactor-Cr-WS}}$  ( $T_L = 1300$  K).

$T_H$ (K)	$\dot{Q}_{\text{cooler-1-Cr-WS}}$ (kW)	$\dot{Q}_{\text{cooler-2-Cr-WS}}$ (kW)	$\dot{Q}_{\text{cooler-3-Cr-WS}}$ (kW)	$\dot{Q}_{\text{splitting-reactor-Cr-WS}}$ (kW)
1800	76.4	0.7	1.2	4.9
1820	87.4	1.2	2.2	9.1
1840	98.5	1.8	3.1	13.2
1860	109.5	2.3	4.1	17.4
1880	120.5	2.9	5.1	21.5
1900	131.6	3.4	6.1	25.6
1920	142.6	4.0	7.1	29.8
1940	175.5	6.0	10.7	44.9
1960	264.9	11.7	21.0	88.3
1980	354.2	17.5	31.3	131.6
2000	441.9	23.1	41.5	174.3
2020	530.2	28.8	51.7	217.3
2040	622.0	34.8	62.4	262.1
2060	709.3	40.4	72.5	304.8
2080	799.2	46.3	83.0	348.8
2100	819.5	47.5	85.2	357.9
2120	827.7	47.9	85.9	360.9
2140	834.5	48.2	86.4	363.3
2160	842.5	48.6	87.1	366.2
2180	851.4	49.0	88.0	369.6
2200	859.5	49.4	88.7	372.6
2220	867.3	49.8	89.3	375.4
2230	871.9	50.0	89.8	377.2

**Fig. 7.** Effect of  $T_H$  on  $\dot{Q}_{\text{FC-Ideal-Cr-WS}}$  and  $\dot{W}_{\text{FC-Ideal-Cr-WS}}$  ( $T_L = 1300$  K).**Fig. 8.** Effect of  $T_H$  on  $\eta_{\text{solar-to-fuel-Cr-WS}}$  ( $T_L = 1300$  K).

period when the  $T_H$  was augmented from 1800 K to 2000 K, the HHV of  $\text{H}_2$  produced has a pronounced influence on the  $\eta_{\text{solar-to-fuel-Cr-WS}}$  was compared to the increase in the  $\dot{Q}_{\text{solar-cycle-Cr-WS}}$ . In contrast, the  $\dot{Q}_{\text{solar-cycle-Cr-WS}}$  has a dominant effect on the  $\eta_{\text{solar-to-fuel-Cr-WS}}$  when the  $T_H$  was rose from 2000 K to 2230 K and hence a drop in

then  $\eta_{\text{solar-to-fuel-Cr-WS}}$  was realized. Overall it can be concluded that the Cr-WS cycle is capable of attaining the maximum  $\eta_{\text{solar-to-fuel-Cr-WS}}$  equal to 26.4% when the TR-Cr = 46.2%,  $T_H = 2000$  K, and  $T_L = 1300$  K.

For further increment in the  $\eta_{\text{solar-to-fuel-Cr-WS}}$  the heat energy released by the three coolers and the WS reactor was recuperated. The application of heat recuperation was responsible for the reduction in the  $\dot{Q}_{\text{solar-cycle-HR-Cr-WS}}$  as compared to  $\dot{Q}_{\text{solar-cycle-Cr-WS}}$ . This drop in the  $\dot{Q}_{\text{solar-cycle-HR-Cr-WS}}$  resulted in the upsurge in the  $\eta_{\text{solar-to-fuel-Cr-WS}}$ . The total amount of  $\dot{Q}_{\text{recuperable-Cr-WS}}$  was increased by 1305.8 KW when the  $T_H$  was enhanced from 1800 K to 2230 K. This upsurge in  $\dot{Q}_{\text{recuperable-Cr-WS}}$  helped to reduce the  $\dot{Q}_{\text{solar-cycle-HR-Cr-WS}}$  by 166.7 kW, 680.7 kW, 1310.0 kW, and 1388.9 kW when compared to the  $\dot{Q}_{\text{solar-cycle-Cr-WS}}$  at  $T_H = 1900$  K, 2000 K, 2100 K, and 2230 K, respectively (assuming 100% HR). With this decrease in the  $\dot{Q}_{\text{solar-cycle-HR-Cr-WS}}$ , the  $\eta_{\text{solar-to-fuel-Cr-WS}}$  was improved up to 45.8%, 48.3%, 42.2%, and 32.6% at  $T_H = 1900$  K, 2000 K, 2100 K, and 2230 K, respectively. Again, after employing the HR, then  $\eta_{\text{solar-to-fuel-Cr-WS}}$  of the Cr-WS cycle was observed to be the highest (48.3%) at  $T_H = 2000$  K.

As the verification of the thermodynamic analysis, the  $\dot{W}_{\text{FC-Ideal-Cr-WS}}$  calculated by using Eq. (23) is compared to the  $\dot{W}_{\text{FC-Ideal-Cr-WS}}$  estimated as per Eq. (27). As the slope of the line is equal to 1, it is confirmed that the  $\dot{W}_{\text{FC-Ideal-Cr-WS}}$  calculated via solving Eqs. (23) and (27) matches very well. These results further conclude that the results reported in this study are precise. The research group is currently working towards exploring the chromium oxide-based redox reactions for the thermochemical splitting of  $\text{CO}_2$ .

## 5. Summary and conclusions

HSC Chemistry 9.9 software was utilized to perform the thermodynamic analysis of the Cr-WS cycle. The equilibrium analysis indicate that the %TR-Cr was increased in three zones (slow zone-1: 1.3% to 7.9%, fast zone-2: 7.9% up to 94.9%, and slow zone-3: 94.9% up to 100%) when the  $T_H$  was increased from 1800 K to 2230 K. From the delta G analysis it was also understood that the WS reaction via re-oxidation of Cr is feasible at all temperatures below 3000 K. To attain a higher %TR-Cr, the  $T_H$  was increased from 1800 K to 2230 K, which resulted into an increment in the  $\dot{Q}_{\text{Cr}_2\text{O}_3\text{-red(partial)-Cr-WS}}$  and  $\dot{Q}_{\text{H}_2\text{O-heating-Cr-WS}}$  by 1906.2 kW and 245.9 kW. Furthermore, the  $\dot{Q}_{\text{cooler-1-Cr-WS}}$ ,  $\dot{Q}_{\text{cooler-2-Cr-WS}}$ ,  $\dot{Q}_{\text{cooler-3-Cr-WS}}$ , and  $\dot{Q}_{\text{splitting-reactor-Cr-WS}}$

were also increased by 795.5 kW, 49.4 kW, 88.6 kW, and 372.3 kW when the  $T_H$  was augmented from 1800 K to 2230 K. The thermodynamic analysis indicate that  $\eta_{solar-to-fuel-Cr-WS}$  reached the peak value at  $T_H$  equal to 2000 K (TR-Cr = 46.2%) and then started to decrease with the further upsurge in the  $T_H$ . Overall the Cr-WS cycle is capable of attaining the maximum  $\eta_{solar-to-fuel-Cr-WS}$  equal to 26.4% when the TR-Cr = 46.2%,  $T_H$  = 2000 K, and  $T_L$  = 1300 K. With the help of the HR = 100%, the  $\eta_{solar-to-fuel-Cr-WS}$  was improved up to 45.8%, 48.3%, 42.2%, and 32.6% at  $T_H$  = 1900 K, 2000 K, 2100 K, and 2230 K, respectively.

#### CRedit authorship contribution statement

**Rahul R. Bhosale:** Conceptualization, Methodology, Software, Validation, Formal analysis, Investigation, Resources, Data curation, Writing - original draft, Writing - review & editing, Visualization, Project administration, Funding acquisition.

#### Declaration of Competing Interest

The authors declare that they have no known competing financial interests or personal relationships that could have appeared to influence the work reported in this paper.

#### Acknowledgment

This publication was made possible by the NPRP grant (NPRP8-370-2-154) from the Qatar National Research Fund (a member of Qatar Foundation). The statements made herein are solely the responsibility of author(s).

#### References

- [1] Lee C. Energy consumption and GDP in developing countries: a cointegrated panel analysis. *Energy Econ* 2005;27:415–27.
- [2] Bhosale RR, Mahajani VV Kinetics of Absorption of Carbon Dioxide in Aqueous Solution of Ethylaminoethanol Modified with N-methyl-2-pyrrolidone. *Sep Sci Technol* 2013;48:2324–37.
- [3] Bhosale RR, Mahajani VV Kinetics of thermal degradation of renewably prepared amines useful for flue gas treatment. *J Renewable Sustainable Energy* 2013;5:063110.
- [4] Bhosale RR, Kumar A, AlMomani F, et al. CO<sub>2</sub> capture using aqueous potassium carbonate promoted by ethylaminoethanol: a kinetic study. *Ind Eng Chem Res* 2016;55:5238–46.
- [5] Dincer I. Environmental issues: I-energy utilization. *Energy Sources* 2001;23:69–81.
- [6] Sorgulu F, Dincer I. A renewable source based hydrogen energy system for residential applications. *Int J Hydrogen Energy* 2018;43:5842–51.
- [7] Bicer Y, Khalid F. Two-step hydrogen chloride cycle for sustainable hydrogen production: An energy and exergy assessment. *Int J Hydrogen Energy* 2019.
- [8] Kalyva AE, Vagia EC, Konstantopoulos AG, et al. Investigation of the solar hybrid photo-thermochemical sulfur-ammonia water splitting cycle for hydrogen production. *Chem Eng Trans* 2015;45:361–6.
- [9] Steinfeld A. Solar thermochemical production of hydrogen—a review. *Sol Energy* 2005;78:603–15.
- [10] Carrillo RJ, Scheffe JR Advances and trends in redox materials for solar thermochemical fuel production. *Sol Energy* 2017;156:3–20.
- [11] Agrafiotis C, Roeb M, Sattler C A review on solar thermal syngas production via redox pair-based water/carbon dioxide splitting thermochemical cycles. *Renew Sustain Energy Rev* 2015;42:254–85.
- [12] Koepf E, Alkneit I, Wieckert C, Meier A A review of high temperature solar driven reactor technology: 25 years of experience in research and development at the Paul Scherrer Institute. *Appl Energy* 2017;188:620–51.
- [13] Loutzenhiser PG, Steinfeld A Solar syngas production from CO<sub>2</sub> and H<sub>2</sub>O in a two-step thermochemical cycle via Zn/ZnO redox reactions: thermodynamic cycle analysis. *Int J Hydrogen Energy* 2011;36:12141–7.
- [14] Bhosale RR. Thermodynamic efficiency analysis of zinc oxide based solar driven thermochemical H<sub>2</sub>O splitting cycle: effect of partial pressure of O<sub>2</sub>, thermal reduction and H<sub>2</sub>O splitting temperatures. *Int J Hydrogen Energy* 2018;43:14915–24.
- [15] Koepf E, Villamil W, Meier A Pilot-scale solar reactor operation and characterization for fuel production via the Zn/ZnO thermochemical cycle. *Appl Energy* 2016;165:1004–23.
- [16] Chambon M, Abanades S, Flamant G Solar thermal reduction of ZnO and SnO<sub>2</sub>: characterization of the recombination reaction with O<sub>2</sub>. *Chem Eng Sci* 2010;65:3671–80.
- [17] Levêque G, Abanades S. Investigation of thermal and carbothermal reduction of volatile oxides (ZnO, SnO<sub>2</sub>, GeO<sub>2</sub>, and MgO) via solar-driven vacuum thermogravimetry for thermochemical production of solar fuels. *Thermochim Acta* 2015;605:86–94.
- [18] Bhosale RR, Kumar A, Sutar P Thermodynamic analysis of solar driven SnO<sub>2</sub>/SnO based thermochemical water splitting cycle. *Energy Convers Manage* 2017;135:226–35.
- [19] Charvin P, Abanades S, Lemont F, Flamant G. Experimental study of SnO<sub>2</sub>/SnO thermochemical systems for solar production of hydrogen. *AIChE J* 2008;54:2759–67.
- [20] Levêque G, Abanades S Thermodynamic and kinetic study of the carbothermal reduction of SnO<sub>2</sub> for solar thermochemical fuel generation. *Energy Fuels* 2014;28:1396–405.
- [21] Abanades S. CO<sub>2</sub> and H<sub>2</sub>O reduction by solar thermochemical looping using SnO<sub>2</sub>/SnO redox reactions: Thermogravimetric analysis. *Int J Hydrogen Energy* 2012;37:8223–31.
- [22] Scheffe JR, Li J, Weimer AW. A spinel ferrite/hercynite water-splitting redox cycle. *Int J Hydrogen Energy* 2010;35:3333–40.
- [23] Agrafiotis C, Zygogianni A, Pagkoura C, Kostoglou M, Konstantopoulos AG. Hydrogen production via solar-aided water splitting thermochemical cycles with nickel ferrite: Experiments and modeling. *AIChE J* 2013;59:1213–25.
- [24] Shende RV, Puszynski JA, Opoku MK, Bhosale RR Synthesis of novel ferrite foam material for water-splitting application. 2009:978-1.
- [25] Bhosale RR, Shende RV, Puszynski JA Sol-Gel Derived NiFe<sub>2</sub>O<sub>4</sub> Modified with ZrO<sub>2</sub> for Hydrogen Generation from Solar Thermochemical Water-Splitting Reaction. 2012;1387:mrsf11,1387-e09-07.
- [26] Abanades S, Villafan-Vidales HL. CO<sub>2</sub> and H<sub>2</sub>O conversion to solar fuels via two-step solar thermochemical looping using iron oxide redox pair. *Chem Eng J* 2011;175:368–75.
- [27] Bhosale RR, Kumar A, van den Broeke Leo JP, et al. Solar hydrogen production via thermochemical iron oxide–iron sulfate water splitting cycle. *Int J Hydrogen Energy* 2015;40:1639–50.
- [28] Bhosale RR, Kumar A, AlMomani F, et al. Effectiveness of Ni incorporation in iron oxide crystal structure towards thermochemical CO<sub>2</sub> splitting reaction. *Ceram Int* 2017;43:5150–5.
- [29] Bhosale RR, Kumar A, AlMomani F, Alkneit I. Propylene oxide assisted sol-gel synthesis of zinc ferrite nanoparticles for solar fuel production. *Ceram Int* 2016;42:2431–8.
- [30] Bhosale RR, Alkneit I, van den Broeke, Leo LP, et al. Sol-Gel Synthesis of Nanocrystalline Ni-Ferrite and Co-Ferrite Redox Materials for Thermochemical Production of Solar Fuels. 2014;1675:mrss14,1675-rr06-10.
- [31] Bhosale R, Shende R, Puszynski J Sol-gel synthesis of ferrite foam materials for H<sub>2</sub> generation from water-splitting reaction. 2010;1:368.
- [32] Allen KM, Coker EN, Auyeung N, Klausner JF. Cobalt ferrite in YSZ for use as reactive material in solar thermochemical water and carbon dioxide splitting, part I: material characterization. *JOM* 2013;65:1670–81.
- [33] Neises M, Roeb M, Schmücker M, Sattler C, Pitz-Paal R. Kinetic investigations of the hydrogen production step of a thermochemical cycle using mixed iron oxides coated on ceramic substrates. *Int J Energy Res* 2010;34:651–61.
- [34] Scheffe JR, Francés A, King DM, et al. Atomic layer deposition of iron (III) oxide on zirconia nanoparticles in a fluidized bed reactor using ferrocene and oxygen. *Thin Solid Films* 2009;517:1874–9.
- [35] Roeb M, Gathmann N, Neises M, Sattler C, Pitz-Paal R. Thermodynamic analysis of two-step solar water splitting with mixed iron oxides. *Int J Energy Res* 2009;33:893–902.
- [36] Chueh WC, Haile SM. A thermochemical study of ceria: exploiting an old material for new modes of energy conversion and CO<sub>2</sub> mitigation. *Philos Trans A Math Phys Eng Sci* 2010;368:3269–94. <https://doi.org/10.1098/rsta.2010.0114> [doi].
- [37] Muhich CL, Evanko BW, Weston KC, et al. Efficient generation of H<sub>2</sub> by splitting water with an isothermal redox cycle. *Science* 2013;341:540–2. <https://doi.org/10.1126/science.1239454> [doi].
- [38] Scheffe JR, Jacot R, Patzke GR, Steinfeld A. Synthesis, Characterization, and Thermochemical Redox Performance of Hf<sub>4</sub>, Zr<sub>4</sub>, and Sc<sub>3</sub> Doped Ceria for Splitting CO<sub>2</sub>. *J Phys Chem C* 2013;117:24104–14.
- [39] Bhosale RR, Takalkar G, Sutar P, Kumar A, AlMomani F, Khraisheh M. A decade of ceria based solar thermochemical H<sub>2</sub>O/CO<sub>2</sub> splitting cycle. *Int J Hydrogen Energy* 2019;44:34–60.
- [40] Bhosale RR, Kumar A, AlMomani F, et al. Assessment of CexZryHfzO<sub>2</sub> based oxides as potential solar thermochemical CO<sub>2</sub> splitting materials. *Ceram Int* 2016;42:9354–62.
- [41] Bhosale RR, Kumar A, AlMomani F, Alkneit I. Sol-gel derived CeO<sub>2</sub>-Fe<sub>2</sub>O<sub>3</sub> nanoparticles: Synthesis, characterization and solar thermochemical application. *Ceram Int* 2016;42:6728–37.
- [42] Takalkar G, Bhosale R, Kumar A, et al. Transition metal doped ceria for solar thermochemical fuel production. *Sol Energy* 2018;172:204–11.
- [43] Bhosale R, Takalkar G Nanostructured co-precipitated CeO<sub>2</sub>. 9LnO<sub>3</sub>. 1O<sub>2</sub> (Ln = La, Pr, Sm, Nd, Gd, Tb, Dy, or Er) for thermochemical conversion of CO<sub>2</sub>. *Ceram Int* 2018;44:16688–97.
- [44] Furler P, Scheffe JR, Steinfeld A. Syngas production by simultaneous splitting of H<sub>2</sub>O and CO<sub>2</sub> via ceria redox reactions in a high-temperature solar reactor. *Energy Environ Sci* 2012;5:6098–103.
- [45] Bader R, Venstrom LJ, Davidson JH, Lipiński W. Thermodynamic analysis of isothermal redox cycling of ceria for solar fuel production. *Energy Fuels* 2013;27:5533–44.
- [46] Venstrom LJ, De Smith RM, Hao Y, Haile SM, Davidson JH. Efficient splitting of CO<sub>2</sub> in an isothermal redox cycle based on ceria. *Energy Fuels* 2014;28:2732–42.
- [47] Le Gal A, Abanades S, Bion N, Le Mercier T, Harlé V. Reactivity of doped ceria-

- based mixed oxides for solar thermochemical hydrogen generation via two-step water-splitting cycles. *Energy Fuels* 2013;27:6068–78.
- [48] Scheffe JR, Weibel D, Steinfeld A. Lanthanum–strontium–manganese perovskites as redox materials for solar thermochemical splitting of H<sub>2</sub>O and CO<sub>2</sub>. *Energy Fuels* 2013;27:4250–7.
- [49] Takalkar G, Bhosale RR. Solar thermocatalytic conversion of CO<sub>2</sub> using Pr<sub>x</sub>Sr (1–x) MnO<sub>3</sub> –  $\delta$  perovskites. *Fuel* 2019;254:115624.
- [50] Demont A, Abanades S. High redox activity of Sr-substituted lanthanum manganite perovskites for two-step thermochemical dissociation of CO<sub>2</sub>. *RSC Adv* 2014;4:54885–91.
- [51] Takalkar G, Bhosale R, AlMomani F. Combustion synthesized A<sub>0.5</sub>Sr<sub>0.5</sub>MnO<sub>3- $\delta$</sub>  perovskites (where, a = La, Nd, Sm, Gd, Tb, Pr, Dy, and Y) as redox materials for thermochemical splitting of CO<sub>2</sub>. *Appl Surf Sci* 2019.
- [52] Bhosale RR, Kumar A, Ashok A, et al. La-based perovskites as oxygen-exchange redox materials for solar syngas production. *MRS Adv* 2017;2:3365–70.
- [53] Demont A, Abanades S, Beche E. Investigation of perovskite structures as oxygen-exchange redox materials for hydrogen production from thermochemical two-step water-splitting cycles. *J Phys Chem C* 2014;118:12682–92.
- [54] Dey S, Naidu B, Govindaraj A, Rao C. Noteworthy performance of La<sub>1-x</sub>Ca<sub>x</sub>MnO<sub>3</sub> perovskites in generating H<sub>2</sub> and CO by the thermochemical splitting of H<sub>2</sub>O and CO<sub>2</sub>. *PCCP* 2015;17:122–5.
- [55] Takacs M, Hoes M, Caduff M, Cooper T, Scheffe JR, Steinfeld A. Oxygen non-stoichiometry, defect equilibria, and thermodynamic characterization of LaMnO<sub>3</sub> perovskites with Ca/Sr A-site and Al B-site doping. *Acta Mater* 2016;103:700–10.
- [56] Carrillo RJ, Scheffe JR. Beyond Ceria: Theoretical Investigation of Isothermal and Near-Isothermal Redox Cycling of Perovskites for Solar Thermochemical Fuel Production. *Energy Fuels* 2019.
- [57] Bhosale RR, Kumar A, AlMomani F, Ghosh U, Khraisheh M. A comparative thermodynamic analysis of samarium and erbium oxide based solar thermochemical water splitting cycles. *Int J Hydrogen Energy* 2017;42:23416–26.
- [58] Bhosale R, Kumar A, AlMomani F, et al. Solar Hydrogen Production via a Samarium Oxide-Based Thermochemical Water Splitting Cycle. *Energies* 2016;9:316.
- [59] Bhosale RR, Sutar P, Kumar A, et al. Solar hydrogen production via erbium oxide based thermochemical water splitting cycle. *J Renewable Sustainable Energy* 2016;8:034702.
- [60] Bhosale R, Kumar A, AlMomani F. Solar thermochemical hydrogen production via terbium oxide based redox reactions. *Int J Photoenergy* 2016;2016.
- [61] Banerjee A, Pai M, Bhattacharya K, et al. Catalytic decomposition of sulfuric acid on mixed Cr/Fe oxide samples and its application in sulfur–iodine cycle for hydrogen production. *Int J Hydrogen Energy* 2008;33:319–26.
- [62] Kerkez-Kuyumcu Ö, Kibar E, Dayıoğlu K, Gedik F, Akın AN, Özkara-Aydinoğlu Ş. A comparative study for removal of different dyes over M/TiO<sub>2</sub> (M = Cu, Ni, Co, Fe, Mn and Cr) photocatalysts under visible light irradiation. *J Photochem Photobiol A* 2015;311:176–85.
- [63] Singh P, Hegde M. Ce<sub>0.67</sub>Cr<sub>0.33</sub>O<sub>2.11</sub>: A new low-temperature O<sub>2</sub> evolution material and H<sub>2</sub> generation catalyst by thermochemical splitting of water. *Chemistry of Materials* 2010;22:762–8.
- [64] Le Gal A, Abanades S. Catalytic investigation of ceria-zirconia solid solutions for solar hydrogen production. *Int J Hydrogen Energy* 2011;36:4739–48.